

Thermodynamic investigations on the growth of CuAlO_2 delafossite crystals

Nora Wolff*, Detlef Klimm, and Dietmar Siche

Leibniz-Institut für Kristallzüchtung, Max-Born-Str. 2, 12489 Berlin, Germany

Abstract

Simultaneous differential thermal analysis (DTA) and thermogravimetric (TG) measurements with copper oxide/aluminum oxide mixtures were performed in atmospheres with varying oxygen partial pressures and with crucibles made of different materials. Only sapphire and platinum crucibles proved to be stable under conditions that are useful for the growth of CuAlO_2 delafossite single crystals. Then the ternary phase diagram Al_2O_3 – CuO – Cu and its isopleth section Cu_2O – Al_2O_3 were redetermined. Millimeter sized crystals could be obtained from copper oxide melts with 1–2 mol-% addition of aluminum oxide that are stable in platinum crucibles held in oxidizing atmosphere containing 15–21% oxygen.

Keywords: CALPHAD, differential thermal analysis, Phase diagram, p-type, CuAlO_2

1. Introduction

The technological interest in developing transparent conducting oxide (TCO) or transparent semiconducting oxide (TSO) materials has seen a dramatic increase in recent years. Established TCO's, such as CdO , β - Ga_2O_3 , In_2O_3 , SnO_2 and ZnO [1, 2] are n-type semiconductors in which electrons act as main charge carriers. However, in semiconductor electronics, p-n-junctions are of major importance where hole conduction is required in the p-type parts [3]. P-type TCO's could find their applications in functional p-n heterojunctions for transparent solar cells, ultraviolet-emitting diodes (LED) [4, 5], touch screens, thermoelectric converters and other transparent optoelectronic devices [6]. Unfortunately the valence bands of most oxides are very flat. This impedes high hole mobility which would be important for commercial devices. Some copper(I) compounds, including the delafossite type CuAlO_2 were identified belonging to the small group of prospective p-type TCO's [7].

*Corresponding author

Email address: nora.wolff@ikz-berlin.de (Nora Wolff)

In the ternary delafossite oxide structure of CuAlO_2 {O—Cu—O} dumbbell layers are stacked with AlO_6 octahedra and hexagonal Cu layers perpendicular to the c axis [8]. CuAlO_2 delafossite has trigonal symmetry (space group $R\bar{3}m$), with $a = b = 2.857 \text{ \AA}$, $c = 16.939 \text{ \AA}$, an indirect bandgap of 2.22 eV and a direct gap of 3.4 eV [9].

So far, CuAlO_2 has mainly been grown as polycrystalline thin layers or on a ceramic route [4, 10, 11]. Only scarce reports on the growth of small single crystal can be found in the literature [8, 9, 12, 13] and all of them rely on crystallization from melt solutions based on excess copper oxides (Cu_2O , CuO) and Al_2O_3 . This results in millimeter-sized (0001) platelets with several $100 \mu\text{m}$ thickness. It is surprising that on the one hand recent authors used often both Cu_2O and CuO as components of the flux, but on the other hand not much attention is given to the growth atmosphere. Via the reaction



both copper oxides are in equilibrium. The enthalpy of the exothermal oxidation (1) as calculated with the FactSage integrated thermodynamic databank system [14] changes almost linearly from -142 kJ/mol at 0°C to -129 kJ/mol at 1200°C which means that high temperature T and low oxygen fugacity (expressed as partial pressure p_{O_2}) shift (1) to the educt side with copper(I) oxide.

Over a wide range of experimental conditions (T, p_{O_2}), covering all conditions that are used in this study, aluminum occurs exclusively as Al^{3+} , and hence Al_2O_3 can be considered as a component of the system. $2 \text{CuAlO}_2 = \text{Cu}_2\text{O} \cdot \text{Al}_2\text{O}_3$ is the 1:1 intermediate compound in the pseudobinary system $\text{Cu}_2\text{O}-\text{Al}_2\text{O}_3$. However, via (1) CuO will be present in the system, and can form with Al_2O_3 the spinel phase CuAl_2O_4 [15]. It will be shown later that under certain experimental conditions also metallic copper can be formed, and consequently the concentration triangle $\text{Al}_2\text{O}_3-\text{CuO}-\text{Cu}$ in Fig. 6a) will be used in this paper to discuss growth conditions for CuAlO_2 delafossite crystals.

In a report on the separate systems $\text{CuO}-\text{Al}_2\text{O}_3$ and $\text{Cu}_2\text{O}-\text{Al}_2\text{O}_3$ it was found that the spinel CuAl_2O_4 is stable in air only up to 1000°C and is then converted to CuAlO_2 , which was stable to about 1260°C [16]. Gadalla and White [17] reported the ternary $\text{Al}_2\text{O}_3-\text{CuO}-\text{Cu}_2\text{O}$ for oxygen fugacities $0.21 \leq p_{\text{O}_2}/\text{bar} \leq 1.0$. According to their data, single crystals of CuAlO_2 should crystallize from melts containing 10-20 mol% Al_2O_3 in Cu_2O , which is in slight contrast with the results that will be presented in this study. Nevertheless, their study proposes for $p_{\text{O}_2} = 0.21 \text{ bar}$ peritectic melting of CuAlO_2 at 1238°C to $\alpha\text{-Al}_2\text{O}_3$ and a melt consisting mainly of CuO and Cu_2O , which is in fairly good agreement with the results that will be presented here. For large $p_{\text{O}_2} \approx 0.4 \text{ bar}$, the stability range for the CuAl_2O_4 spinel was found elsewhere [18] to be wider, compared to Gadalla and White [17], but this difference is not relevant for the growth of the copper(I) compound CuAlO_2 .

It is the aim of this work to define experimental conditions (melt composition, atmosphere, temperature regime, crucible material) where CuAlO_2 single crystals can be growth from self-flux. Self-fluxes are expected to result in crys-

tals with less impurities, compared to growth from fluxes containing foreign components, such as hydrothermal solutions, or by sol-gel processes [19, 20, 21].

2. Experimental

Simultaneous differential thermal analysis (DTA) and thermogravimetric (TG) measurements were carried out with a Netzsch STA 409CD. Gas flow was set by a mass flow controller to deliver atmospheres ranging from 100% O₂ to 2% O₂ in Ar, and air. Samples were prepared by mixing powders of Al₂O₃ (Alfa Aesar, 99.997% purity) and Cu₂O (Fox Chemicals, 99.99% purity) to concentrations between pure Cu₂O and 15 mol-% Al₂O₃ in Cu₂O. For all measurements a temperature program was selected, which resembles the conditions during a real crystal growth run. With this program, it was possible to test potential crucible materials for their steadiness and to obtain some first information about redox processes of copper oxides. The powder mixtures were heated in crucibles with a rate of 5 K/min to 1200 or 1300 °C (3 h dwell time) then slowly cooled down with 3 K/min to 900 °C and 1.5 K/min to 100 °C. The dwell time of 3 h was chosen to test the stability of the respective crucible material. In order to ensure that the CuAlO₂ phase was formed, the temperature program was run twice.

The phase compositions of all samples were characterized by X-ray powder diffraction with a GE Inspection Technologies XRD 3003 TT (Bragg Brentano geometry and Cu K α radiation).

The CuAlO₂ composition of the crystals was proven by X-ray fluorescence spectroscopy.

3. Results and discussion

First measurements gave information on the oxidation and reduction behavior of copper(I)oxide. If Cu₂O (pure or mixed with Al₂O₃) was heated in an atmosphere containing O₂, oxidation to CuO occurred around 350 °C, which is in agreement with Gadalla and White [17]. DTA-peaks between 1000 °C and 1050 °C result from endothermal melt processes and also from endo- or exothermal redox processes between Cu⁺ and Cu²⁺ (1). An oxidation process is connected with a mass increase in the associated TG curve, together with an exothermal DTA effect. A reduction is connected with a mass decrease because of oxygen release, and is endothermal. This is demonstrated by the red curves in Fig. 1 which were obtained with pure Cu₂O. The first three endothermal peaks are connected with a mass loss that is monotonous but changes in rate: E.g. at point (1) where the DTA curve is less endothermal, also the TG curve is flatter. Obviously the reaction rate is smaller at this point, and consequently mass loss is reduced, in agreement with a smaller endothermal effect. The reduction process CuO \rightarrow Cu₂O is completed after the large sharp peak, at point (2) where the sample is still solid. A small exothermal effect after this point and a mass gain of almost 1% starting there indicates that Cu₂O begins re-oxidizing

partially back to CuO. This is surprising because according to Fig. 3 under constant p_{O_2} a higher T should result in lower rather than in higher valence. Obviously, the energy gain resulting from liquid mixture formation, in analogy to (2), is the driving force for the re-oxidation. With increasing CuO content the sample can melt, giving rise to the following broad peak. Visual inspection of samples that were heated up to 1200 °C proved this.

An identical measurement with a Cu₂O/Al₂O₃ mixture (black curves in Fig. 1) is similar, but shows an additional endothermic peak between 1230 °C and 1250 °C. It will be shown later that this peak can be assigned to the peritectic melting of CuAlO₂.

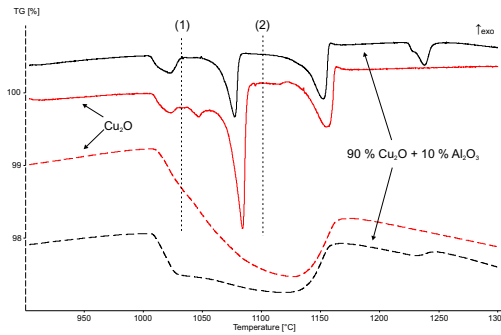


Figure 1: DTA (solid) and TG curves (dashed) between 900 °C and 1300 °C for pure Cu₂O and a 90/10 mixture with Al₂O₃. The DTA peaks between 1000 °C and 1150 °C are overlapped by redox processes (1) (mass change in TG curve).

In further experiments different crucible materials in combination with varying oxygen fugacities in the atmosphere were tested. Ceramic crucibles, for example Al₂O₃, Y₂O₃ [22] or MgO, were infiltrated by copper oxide flux and could be used only in the low- T range where the whole sample remains solid. This is in agreement with a recent report [23] where wetting of alumina surfaces by CuO_{*x*} melts could be reduced only for very low p_{O_2} . In contrast to ceramic Al₂O₃, single crystalline sapphire crucibles proved satisfactorily stable against melts containing CuO_{*x*}. After several days, only minor attack to the crucible surface was visible. But if the melt sticks tightly to them, thermo-mechanical shock can lead to cracking upon cooling. Nevertheless, they could be used if handled with care. Unfortunately, gold crucibles that were used up to 975 °C for the growth of YBa₂Cu₃O_{7-*x*} [24] are not a valid alternative because growth temperatures for the current process are too high. Finally, platinum proved to be the most stable crucible material and was used for all further experiments.

The behavior of Pt crucibles in relation to the copperoxide-rich melt depends mainly on the oxygen fugacity of the growth atmosphere, as shown in Fig. 2. These measurements were performed with identical temperature program but in atmospheres with different p_{O_2} . During the dwell time (3 h at 1200 °C) the sample mass decreased with a rate that became larger for smaller p_{O_2} in the atmosphere, and it will be shown that reduction of copper oxides to metallic

copper is the origin of this effect. For $p_{\text{O}_2} < 0.15$ bar the crucibles were destroyed after the experiment by alloy formation of Pt with Cu.

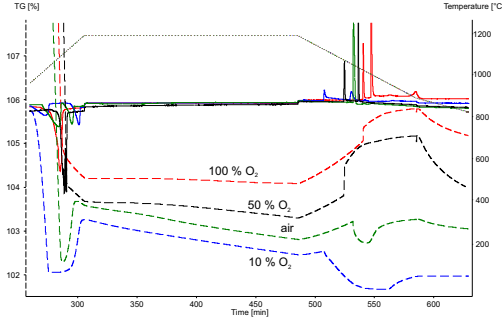


Figure 2: TG (dashed) DTA (solid) curves of measurements with different oxygen partial pressure in a time range between heating (from 900 °C on) and cooling (to 800 °C). During the dwell time at 1200 °C the mass loss increases with lower oxygen content (formation of Cu). With higher oxygen content in the atmosphere (here 50% and 100%) the spinel type CuAl_2O_4 crystallizes instead of CuAlO_2

Problems occurring with CuO_x melts in Pt crucibles were already reported by several authors, e.g. [25, 26] and are related to the formation of solid solutions between Pt and Cu. Both metals crystallize in *fcc* structure and the binary phase diagram Cu–Pt is in the high T range > 1000 °C almost ideal. Only below ≈ 880 °C two intermediate compounds with approximate composition CuPt and Cu_3Pt are stable [27]. For the process temperatures of 1200 – 1300 °C (1473 – 1573 K) that were used in this study, one obtains for a solution of two components (such as Cu and Pt) a maximum ideal Gibbs free energy of mixing at a molar fraction $x = 0.5$, which amounts to

$$\Delta G_{\text{id,mix}} = RT \ln x = -8.5 \dots 9.1 \text{ kJ/mol} \quad (2)$$

(R – gas constant). The energy gain that is given by (2) results in an unfavored stabilization of solid or liquid intermetallic (Cu/Pt) solutions with respect to $\text{CuO}_x + \text{Pt}$. This is demonstrated in Fig. 3 where the solid lines describe the stability phase fields of the copper oxides in a Pt crucible. (The diagram was calculated with FactSage [14]. Pt melting at 1770 °C is out of scale.) The upper border of this figure corresponds to 1 bar O_2 , and the figure demonstrates that for low T and high p_{O_2} $\text{CuO}(\text{s})$ is stable in Pt crucibles. Towards the bottom right corner Cu_2O and subsequently Cu metal are formed. The vertical straight lines are the melting points of these compounds.

The assumption that $\text{Cu}(\text{liq})$ could reside in a $\text{Pt}(\text{s})$ crucible (bottom right phase field) is unrealistic; instead an alloy will be formed. Ideal miscibility in both solid and liquid phases results in the phase boundaries that are drawn as dashed red lines. The two vertical dashed lines limiting the “id-ss+id-melt” phase field correspond to the solidus and liquidus of the Cu–Pt binary system and are in Fig. 3 ca. 200 K lower than in the literature [27], but the width of

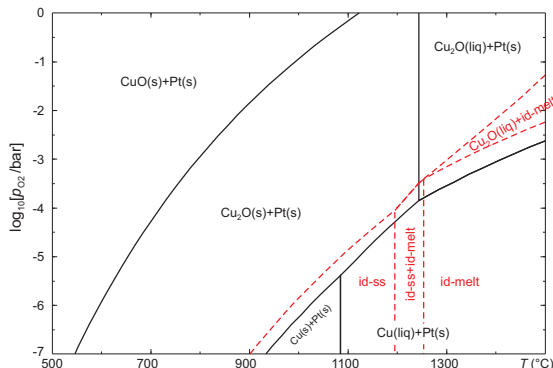


Figure 3: Predominance diagram of the system Cu–Pt–O₂ in coordinates $T, \log[p_{\text{O}_2}]$. Solid black lines: assumption of pure phases CuO(s), Cu₂O(s,liq), Cu(s,liq), Pt(s). Dashed red lines: Pt and Cu are assumed to form ideal solutions in the solid and liquid phases (id-ss and id-melt, respectively).

the two-phase region is realistic. The general trend that phase fields containing pure (not alloyed) Pt(s) will shrink, is not influenced by this difference. One can assume that the identical crystal structure of Cu and Pt, connected with infinite mutual solubility, is the main reason for the instability of CuO_x melt in Pt crucibles. After a sufficiently large number of heating/cooling cycles (ca. 6–8) CuO_x loses its oxygen completely under the formation of (Pt,Cu) alloy, which results finally in crucible destruction. It is especially important that local overheating near the crucible wall is avoided, because the upper boundary of the “Cu₂O+id-melt” phase field approaches quickly very high p_{O_2} were the crucible metal cannot be stabilized even under highly oxidizing conditions.

In Fig. 2 the TG signal shows also mass changes during crystallization near 1000 °C. For the measurements that were performed in the 10% O₂ atmosphere or in air, a mass loss occurs. This can be attributed to the crystallization of CuAlO₂, which is a Cu⁺ compound — in contrast to the melt that contains Cu⁺ and Cu²⁺. For the 50% and 100% curves, however, the sample mass increases during crystallization, which results from the formation of CuAl₂O₄. X-ray powder diffractometry of both types of samples proved the existence of the corresponding copper aluminum oxides. The crossover between spinel and delafossite crystallization is at 25% O₂. 15–21% O₂ are the optimum compromise between crystallization of spinel at too high p_{O_2} , and the formation of too much metallic copper at lower p_{O_2} .

CuAlO₂ is reported to melt under peritectic decomposition to α -Al₂O₃ and a melt with copper oxide excess [16, 17, 18]. For crystal growth experiments it is hence useful, to construct a pseudobinary system Cu₂O–Al₂O₃ and to find the range between the eutectic and peritectic points where delafossite should crystallize first from the melt. This was done in Fig. 4 by adding different amounts of Al₂O₃ to Cu₂O.

For pure Cu₂O and the sample with 2% Al₂O₃ added the melting process is

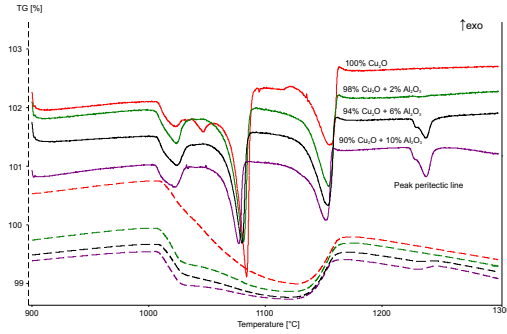


Figure 4: From top to bottom: TG (dashed)/DTA (solid) curves of pure Cu_2O and of mixtures with increased additions of Al_2O_3 (measurements in air).

finished at 1170°C . Not so for the samples with 6% and 10% Al_2O_3 . Another endothermic peak appears around $T_{\text{per}} \approx 1230 - 1250^\circ\text{C}$, and this can be assigned to the peritectic melting of CuAlO_2 . It is interesting to note that also this melting event is connected with a small mass gain, which can be explained as follows: depending on T and p_{O_2} , a certain $\text{Cu}_2\text{O}/\text{CuO}$ ratio is in equilibrium. Below T_{per} , CuAlO_2 , Cu_2O , and CuO are in present. If CuAlO_2 , which contains only Cu^+ melts, more Cu_2O is added, and to maintain equilibrium, a certain amount of it must be oxidized to CuO – which is the origin of the mass gain.

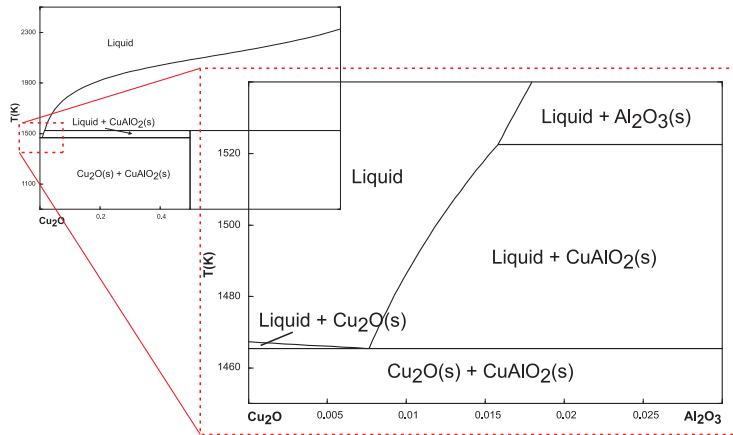


Figure 5: $\text{Cu}_2\text{O}-\text{Al}_2\text{O}_3$ pseudobinary section for $p_{\text{O}_2} = 0.21$ bar, with an enlarged image of the CuAlO_2 liquidus.

Data from the FactSage [14] database and from the literature [17, 28] for CuAlO_2 , CuAl_2O_4 , $\text{CuO}(\text{liq})$, and of the $\text{CuO}_x-\text{Al}_2\text{O}_3$ melt were refined to describe the experimental findings that are reported here, and the pseudobinary section of the phase diagram was obtained (Fig. 5). The eutectic point is ex-

tremely near to CuO_x , close to 1% Al_2O_3 . From there the CuAlO_2 liquidus spans to ca. 2% Al_2O_3 , which represents the growth window for this delafossite phase. It should be noted that Fig. 5 does not represent a binary phase diagram rather than an isopleth section through the concentration triangle that is shown in Fig. 6, because every melting/crystallization process is accompanied by mass changes and hence by shifts of the $\text{Cu}_2\text{O}/\text{CuO}$ ratio.

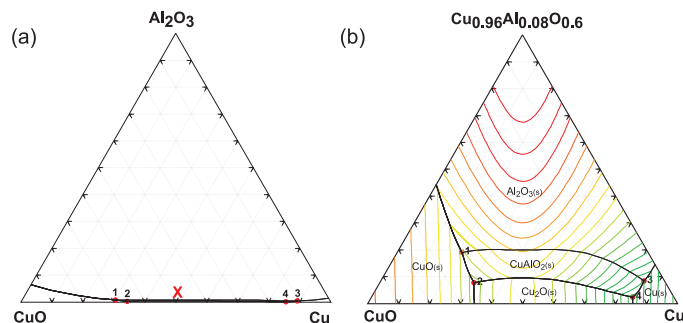


Figure 6: Ternary phase diagram Al_2O_3 - Cu - CuO (a) and its lower part $\text{Cu}_{0.96}\text{Al}_{0.08}\text{O}_{0.6}$ - Cu - CuO (b). Isotherms in triangle (b) are drawn every 50 K; the coldest invariant point 4 is at 1170 K. The $\text{Cu}_{0.96}\text{Al}_{0.08}\text{O}_{0.6}$ point is marked as red X in the Al_2O_3 - Cu - CuO system. The labels for all intermediate phases in a) are written in brackets.

Fig. 6a) describes the system as concentration triangle Al_2O_3 - CuO - Cu . The primary crystallization field of α - Al_2O_3 covers a huge region on top of the triangle, in agreement with Fig. 5. Fig. 6b) is an enlargement of the lowermost part of the triangle, with apex at the position of the star in Fig. 6a). The small crystallization field of $\text{CuAlO}_2(\text{s})$ between Cu_2O and $\text{Al}_2\text{O}_3(\text{s})$ becomes visible which is limited on the right hand side (very reducing conditions) by $\text{Cu}(\text{s})$. As shown in Fig. 3 this field is expected to extend more to the left if one takes into account the alloy formation with Pt as a possible fourth component. At the invariant points 2,3, and 4 the neighboring phases that crystallize first are in equilibrium with the melt. CuAl_2O_4 spinel can be found only in the vicinity of point 1 but transforms in the subsolidus back to CuAlO_2 . The spinel can be formed only under oxygen rich conditions where CuO is also stable, and an extended field of primary crystallization of CuAl_2O_4 was not identified.

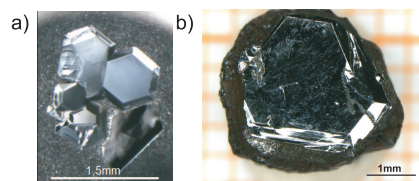


Figure 7: CuAlO_2 crystals grown from Cu_2O solutions with 2 mol-% Al_2O_3 in Pt crucibles in air. a) Spontaneous crystallization in a DTA crucible. b) Spontaneous crystallization in a batch furnace.

Already in the solidified DTA samples where 2 mol-% Al_2O_3 was added to Cu_2O in Pt crucibles, first CuAlO_2 crystals were found that are shown in Fig. 7a). Another test, aimed on checking the long term stability of Pt crucibles against the copper oxide melt was performed in a batch furnace in air. It was found that crucibles with diameters of several centimeters were stable up to seven days. The solidified melt contained CuAlO_2 crystals that were formed by spontaneous crystallization, with sizes up to 5 mm (Fig. 7b).

4. Conclusions

Oxide melts rich in copper oxide can be held stable in platinum crucibles that contain a sufficient oxygen concentration; 15–21% are the lower limit. If p_{O_2} is too low, copper oxides are reduced to the metal, because metallic copper is then stabilized by the formation of a solid or liquid solution. CuAlO_2 crystallizes first from CuO_x melts containing 1–2 mol-% Al_2O_3 , which offers the possibility to grow delafossite crystals from a self-flux without foreign additives. Every melting/crystallization step in this system is connected with a chemical reaction that leads to the absorption or release of oxygen.

Acknowledgments

A. Kwasniewski is thanked for performing X-ray powder analysis and C. Guguschev for performing X-ray fluorescence spectroscopy. We express our gratitude to J. Rehm, I. Schulze-Jonack, E. Thiede and O. Reetz for support in the laboratory, and S. Ganschow for helpful discussions.

The authors acknowledge the funding by the German Research Foundation (DFG) under the project No. SI 463/9-1.

References

- [1] Z. Galazka, Growth Measures to Achieve Bulk Single Crystals of Transparent Semiconducting and Conducting Oxides, in: P. Rudolph (Ed.), Handbook of Crystal Growth (Second Edition), Elsevier, Boston, 2015, pp. 209–240. doi:10.1016/B978-0-444-63303-3.00006-7.
- [2] D. Klimm, Electronic materials with a wide band gap: recent developments, IUCrJ 1 (2014) 281–290. doi:10.1107/S2052252514017229.
- [3] C. Schulz, S. Ulrich, B. Szyszka, p-TCOs für transparente Elektronik, Vakuum in Forschung und Praxis – VIP Journal 24 (4) (2012) 12–16, in German. doi:10.1002/vipr.201200496.
- [4] H. Kawazoe, M. Yasukawa, H. Hyodo, M. Kurita, H. Yanagi, H. Hosono, p-type electrical conduction in transparent thin films of CuAlO_2 , Nature 389 (1997) 939–942. doi:10.1038/40087.

- [5] A. N. Banerjee, S. Nandy, C. K. Ghosh, K. K. Chattopadhyay, Fabrication and characterization of all-oxide heterojunction p-CuAlO_{2+x}/n-Zn_{1-x}Al_xO transparent diode for potential application in “invisible electronics”, *Thin Solid Films* 515 (2007) 7324–7330. doi:10.1016/j.tsf.2007.02.087.
- [6] Q.-J. Liu, Z.-T. Liu, Theoretical insights into structural-electronic relationships and relative stability of the Cu-, Al- and O-terminated CuAlO₂(0001) surfaces, *Vacuum* 107 (2014) 90–98. doi:10.1016/j.vacuum.2014.04.009.
- [7] G. Hautier, A. Miglio, G. Ceder, G.-M. Rignanese, X. Gonze, Identification and design principles of low hole effective mass p-type transparent conducting oxides, *Nature communications* 4 (2013) 2292. doi:10.1038/ncomms3292.
- [8] M. S. Lee, T. Y. Kim, D. Kim, Anisotropic electrical conductivity of delafossite-type CuAlO₂ laminar crystal, *Applied Physics Letters* 79 (2001) 2028–2030. doi:10.1063/1.1405809.
- [9] J. S. Yoon, Y. S. Nam, K. S. Baek, C. W. Park, H. L. Ju, and S. K. Chang, Growth and properties of transparent conducting CuAlO₂ single crystals by a flux self-removal method, *J. Crystal Growth* 366 (2013) 31–34. doi:10.1016/j.jcrysgro.2012.12.134.
- [10] H. Yanagi, S.-i. Inoue, K. Ueda, H. Kawazoe, H. Hosono, N. Hamada, Electronic structure and optoelectronic properties of transparent p-type conducting CuAlO₂, *J. Appl. Phys.* 88 (2000) 4159. doi:10.1063/1.1308103.
- [11] D. Byrne, A. Cowley, N. Bennett, E. McGlynn, The luminescent properties of CuAlO₂, *J. Materials Chemistry C* 2 (2014) 7859. doi:10.1039/C4TC01311E.
- [12] T. Ishiguro, A. Kitazawa, N. Mizutani, M. Kato, Single-crystal growth and crystal structure refinement of CuAlO₂, *J. Solid State Chem.* 40 (1981) 170–174. doi:10.1016/0022-4596(81)90377-7.
- [13] R. Brahimi, G. Rekhila, M. Trari, Y. Bessekhoud, Crystal growth and transport properties of CuAlO₂ single crystal, *Crystallography Reports* 59 (2014) 1088–1092. doi:10.1134/S1063774514070062.
- [14] www.factsage.com, FactSage 7.1, GTT Technologies, Kaiserstr. 100, 52134 Herzogenrath, Germany (2017).
- [15] H. S. O’Neill, M. James, W. a. Dollase, S. a. T. Redfern, Temperature dependence of the cation distribution in CuAl₂O₄ spinel, *European Journal of Mineralogy* 17 (2005) 581–586. doi:10.1127/0935-1221/2005/0017-0581.

- [16] S. K. Misra, A. C. D. Chaklader, The system copper oxide–alumina, *Journal of the American Ceramic Society* 46 (1963) 509–509. doi:10.1111/j.1151-2916.1963.tb13788.x.
- [17] A. M. M. Gadalla, J. White, Equilibrium relationships in the system CuO–Cu₂O–Al₂O₃, *Trans. Brit. Ceram. Soc.* 63 (1964) 39–62.
- [18] K. T. Jacob, C. B. Alcock, Thermodynamics of CuAlO₂ and CuAl₂O₄ and phase equilibria in the system Cu₂O–CuO–Al₂O₃, *Journal of the American Ceramic Society* 58 (1975) 192–195. doi:10.1111/j.1151-2916.1975.tb11441.x.
- [19] T. Sato, K. Sue, H. Tsumatori, M. Suzuki, S. Tanaka, A. Kawai-Nakamura, K. Saitoh, K. Aida, T. Hiaki, Hydrothermal synthesis of CuAlO₂ with the delafossite structure in supercritical water, *The Journal of Supercritical Fluids* 46 (2008) 173 – 177. doi:http://dx.doi.org/10.1016/j.supflu.2008.04.002.
- [20] D. Y. Shahriari, A. Barnabè, T. O. Mason, K. R. Poeppelmeier, A high-yield hydrothermal preparation of CuAlO₂, *Inorganic Chemistry* 40 (2001) 5734–5735. doi:10.1021/ic015556h.
- [21] S. Götzendörfer, Synthesis of copper-based transparent conductive oxides with delafossite structure via sol-gel processing, Ph.D. thesis, Julius-Maximilians-Universität, Würzburg (2010).
- [22] Y. Yamada, Y. Shiohara, Continuous crystal growth of YBa₂Cu₃O_{7-x} by the modified top-seeded crystal pulling method, *Physica C: Superconductivity* 217 (1993) 182–188. doi:http://dx.doi.org/10.1016/0921-4534(93)90810-D.
- [23] M. Diemer, A. Neubrand, K. P. Trumble, J. Rödel, Influence of oxygen partial pressure and oxygen content on the wettability in the copper–oxygen–alumina system, *J. American Ceramic Soc.* 82 (1999) 2825–2832. doi:10.1111/j.1151-2916.1999.tb02163.x.
- [24] Y. K. Tao, H. C. Chen, L. Martini, J. Bechtold, Z. J. Huang, P. H. Hor, Crystal growth of YBa₂Cu₃O_{7-x} and reaction of gold crucible with Ba-Cu-rich flux, *J. Crystal Growth* 114 (1991) 279–282. doi:10.1016/0022-0248(91)90041-3.
- [25] D. Schultze, Applications of differential thermal analysis to the preparation of single crystals, *thermochimica acta* 190 (1991) 77–110. doi:10.1016/0040-6031(91)87140-R.
- [26] S. Mudenda, G. M. Kale, Y. R. S. Hara, Rapid synthesis and electrical transition in p-type delafossite CuAlO₂, *J. Mater. Chem. C* 2 (2014) 9233–9239. doi:10.1039/C4TC01349B.

- [27] T. Abe, B. Sundman, H. Onodera, Thermodynamic assessment of the Cu–Pt system, *J. of Phase Equilibria and Diffusion* 27 (2006) 5–13. doi:10.1361/105497196X92736.
- [28] L. Schramm, G. Behr, W. Löser, K. Wetzig, Thermodynamic reassessment of the Cu–O phase diagram, *J. Phase Equilib. Diff.* 26 (2005) 605–612. doi:10.1361/154770305X74421.